ON THE NORMAL STRESSES IN THE ELASTIC BODY WITH PERIODICALLY CURVED ROW FIBRES

Reşat KÖŞKER[*], Yasemen UÇAN

Yıldız Teknik Üniversitesi, Kimya-Metalurji Fakültesi, Matematik Mühendisliği Bölümü, Yıldız-İSTANBUL

ABSTRACT

Within the framework of the piecewise homogeneous body model with the use of the three-dimensional equations of the theory of elasticity for anisotropic body a method that is developed to investigate the stress distribution in the infinite elastic matrix containing a periodically curved row fibres having a sine-phase is used to investigate related normal stresses. It is assumed that the materials of the fibres are the same and midlines of these fibres are in the same plane. Under uniaxial loading along the fibres the normal stresses acting along the fibers at interface points are investigated. The influences of the problem parameters on these stresses are analyzed. The corresponding numerical results are presented.

Keywords: Unidirectional fibrous composite, row fibers, curved composite, normal stresses.

PERİYODİK EĞRİLİKLİ SIRALI LİFLER İÇEREN ELASTİK ORTAMDAKİ NORMAL GERİLMELER HAKKINDA

ÖZET

Aynı fazlı periyodik eğrilikli sıralı lifler içeren sonsuz elastik matristeki gerilme yayılımını araştırmak için parçalı homojen cisim modeli çerçevesinde, izotrop olmayan cisimler için elastisite teorisinin üç-boyutlu denklemleri kullanılarak geliştirilen yöntem, ilgili normal gerilmelerin araştırılmasında kullanılmıştır. Lif malzemelerinin aynı ve bu liflerin orta çizgilerinin aynı düzlemde yerleştikleri varsayılmıştır. Lifler boyunca tek yönlü yüklemeler sonucu, lifler boyunca arayüzey üzerindeki noktalarda etkiyen normal gerilmeler incelenmiştir. Problem parametrelerinin bu gerilmeler üzerindeki etkileri analiz edilmiştir. İlgili sayısal sonuçlar verilmiştir.

Anahtar Sözcükler: Tek yönlü lifli kompozitler, sıralı lifler, eğrilikli kompozit, normal gerilmeler.

1. INTRODUCTION

It is well known that in the structure of the unidirectional fibrous composites in many cases fibres have an initial curving caused by design factors or caused by the action of various factors during technological process [1-3]. According to a large number of theoretical and experimental investigations described in [1-5], this curving can be the cause of the failure (separation of fibres from matrix) under uniaxial tension or compression of the composite along the fibres. Therefore the theoretical investigations of the self-balanced stresses arising as a result of fibre curving have a great significance in the viewpoint of the theoretical and the application sense. For investigating

---

[*] Sorumlu Yazar/Corresponding Autor: e-mail: kosker@yildiz.edu.tr , Tel: (0212) 449 17 29

such a problem within the framework of a piecewise homogeneous body model with the use of the three-dimensional linear theory of elasticity, a method is developed in [6] and the corresponding numerical results are analyzed in [7]. In [8-10] the method [6] is developed for the corresponding problem on the two neighboring fibres in an infinite elastic matrix. Moreover, in [8-10] the corresponding numerical results are analyzed. It is evident that the model consisting of the two neighbouring fibres in an infinite matrix allows us to have some information on the interaction of the curved fibres under determination of the self-balanced stresses. But, in the real cases the interaction of the fibres requires a more complicated model. In connection with this, the following step of the modelling of the location of the fibres in an infinite matrix can be taken as the row fibres. For this purpose, in [12] the approach [8-10] is developed for the periodically located row fibres in the infinite matrix and the numerical results on the self-balanced stresses acting on the interface are analyzed. In the present paper, by the use of the method [12], the normal stresses acting along the fibers at interface points are investigated under uniaxial loading along the fibres.

2. FORMULATION OF THE PROBLEM

We associate Cartesian $O_k x_{k1} x_{k2} x_{k3}$ and cylindrical $O_k r_k \theta_k z_k$ system of coordinates with the midline of each fibre (Figure 1). Here $k = -\infty,...,-2,-1,0,1,2,...,+\infty$ denote the number of fibres.
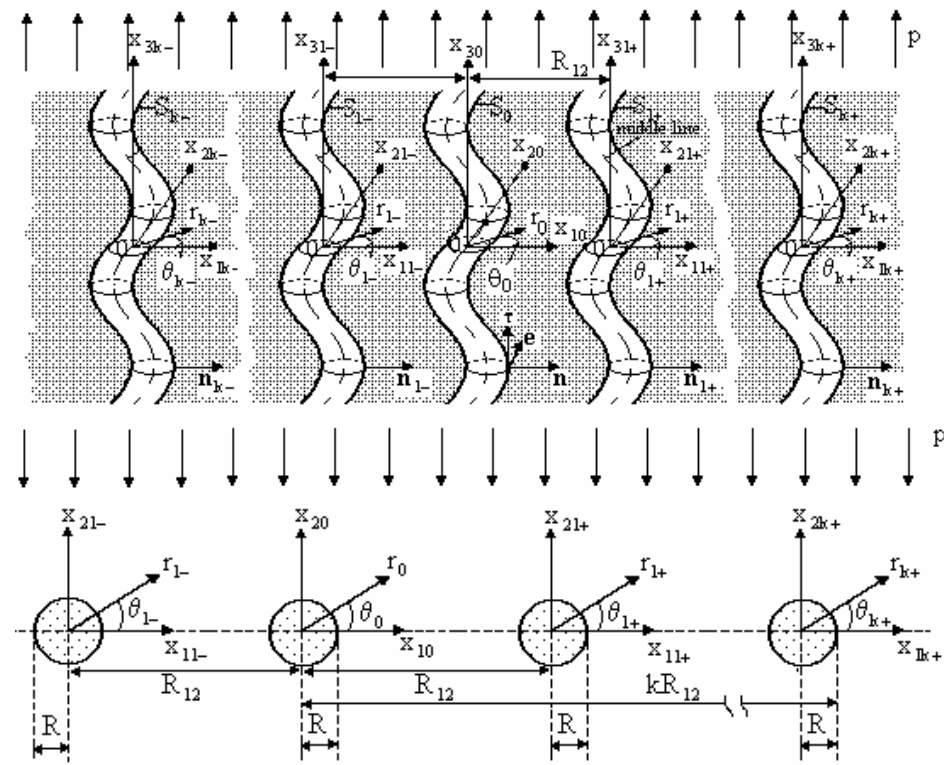
Figure 1. The geometry of the material structure and chosen coordinates

According to Figure 1,

$$x_{2k} = x_{20}, \ x_{3k} = x_{30} = x_3, \ x_{1k} = kR_{12} + x_{10}$$

$$r_0 e^{i\theta_0} = kR_{12} + r_k e^{i\theta_k}, \ z_k = z_0 = z \tag{1}$$

The midlines of the fibres are given by the equations

$$x_{1k} = L\sin(\frac{2\pi}{\ell}x_{3k}), \ x_{2k} = 0 ; \tag{2}$$

and the cross-section of each fibre, which is perpendicular to the midline, is a circle with constant radius *R* along the entire length of the fibres. We assume that, *L* (curving amplitude of the fibre) is smaller than ℓ (curving period) and introduce a small parameter $\varepsilon = L/\ell$, ($0 < \varepsilon << 1$).

According to Eqs. (2), equations of the contact surfaces S_k between the fibres and the matrix and their normal vectors are

$$r_k = R + \sum_{q=1}^{\infty}\varepsilon^q a_{kq}(\theta_k, t_3) , \ z_k = t_3 + \sum_{q=1}^{\infty}\varepsilon^q b_{kq}(\theta_k, t_3), \ n_{kr} = 1 + \sum_{q=1}^{\infty}\varepsilon^q c_{kq}(\theta_k, t_3),$$

$$n_{k\theta} = \sum_{q=1}^{\infty}\varepsilon^q d_{kq}(\theta_k, t_3), \ n_{kz} = \sum_{q=1}^{\infty}\varepsilon^q f_{kq}(\theta_k, t_3) \tag{3}$$

where t_3 ($t_3 \in (-\infty, +\infty)$) is a parameter and explicit expression of the functions $a_{kq}(\theta_k, t_3)$,..., $f_{kq}(\theta_k, t_3)$,... appearing in Eqs. (3) are given in [3].

In what follows, the values related to the fibres will be denoted by the superscripts (2k), but those related to the matrix by the superscript (1). The materials of the fibers and matrix are transversally isotropic with the symmetry axis Ox_3. Thus, in the cylindrical system of coordinates, we can write the following governing field equations:

$$\frac{\partial\sigma_{rr}^{(n)}}{\partial r} + \frac{1}{r}\frac{\partial\sigma_{r\theta}^{(n)}}{\partial\theta} + \frac{\partial\sigma_{rz}^{(n)}}{\partial z} + \frac{1}{r}\left(\sigma_{rr}^{(n)} - \sigma_{\theta\theta}^{(n)}\right) = 0, \quad \frac{\partial\sigma_{r\theta}^{(n)}}{\partial r} + \frac{1}{r}\frac{\partial\sigma_{\theta\theta}^{(n)}}{\partial\theta} + \frac{\partial\sigma_{\theta z}^{(n)}}{\partial z} + \frac{2}{r}\sigma_{r\theta}^{(n)} = 0,$$

$$\frac{\partial\sigma_{rz}^{(n)}}{\partial r} + \frac{1}{r}\frac{\partial\sigma_{\theta z}^{(n)}}{\partial\theta} + \frac{\partial\sigma_{zz}^{(n)}}{\partial z} + \frac{1}{r}\sigma_{rz}^{(n)} = 0, \tag{4}$$

$$\sigma_{rr}^{(n)} = A_{11}^{(n)}\varepsilon_{rr}^{(n)} + A_{12}^{(n)}\varepsilon_{\theta\theta}^{(n)} + A_{13}^{(n)}\varepsilon_{zz}^{(n)}, \ \sigma_{\theta\theta}^{(n)} = A_{12}^{(n)}\varepsilon_{rr}^{(n)} + A_{11}^{(n)}\varepsilon_{\theta\theta}^{(n)} + A_{13}^{(n)}\varepsilon_{zz}^{(n)},$$

$$\sigma_{zz}^{(n)} = A_{13}^{(n)}\varepsilon_{rr}^{(n)} + A_{13}^{(n)}\varepsilon_{\theta\theta}^{(n)} + A_{33}^{(n)}\varepsilon_{zz}^{(n)}, \ \sigma_{rz}^{(n)} = 2G_{13}^{(n)}\varepsilon_{rz}^{(n)}, \sigma_{r\theta}^{(n)} = \left(A_{11}^{(n)} - A_{12}^{(n)}\right)\varepsilon_{r\theta}^{(n)},$$

$$\sigma_{\theta z}^{(n)} = 2G_{13}^{(n)}\varepsilon_{\theta z}^{(n)} \tag{5}$$

$$\varepsilon_{rr}^{(n)} = \frac{\partial u_r^{(n)}}{\partial r}, \ \varepsilon_{\theta\theta}^{(n)} = \frac{\partial u_\theta^{(n)}}{r\partial\theta} + \frac{u_r^{(n)}}{r}, \ \varepsilon_{zz}^{(n)} = \frac{\partial u_z^{(n)}}{\partial z}, \ \varepsilon_{r\theta}^{(n)} = \frac{1}{2}\left(\frac{\partial u_r^{(n)}}{r\partial\theta} + \frac{\partial u_\theta^{(n)}}{\partial r} - \frac{u_\theta^{(n)}}{r}\right),$$

$$\varepsilon_{\theta z}^{(n)} = \frac{1}{2}\left(\frac{\partial u_\theta^{(n)}}{\partial z} + \frac{\partial u_z^{(n)}}{r\partial\theta}\right), \ \varepsilon_{zr}^{(n)} = \frac{1}{2}\left(\frac{\partial u_z^{(n)}}{\partial r} + \frac{\partial u_r^{(n)}}{\partial z}\right). \tag{6}$$

Thus, within the frameworks of each fibre and the matrix Eqs. (4)-(6) are satisfied. In this case, on the interfaces S_k (Figure 1) perfect cohesion is supposedly valid:

$$\left(\sigma_{rr}^{(2k)}n_{kr} + \sigma_{r\theta}^{(2k)}n_{k\theta} + \sigma_{rz}^{(2k)}n_{kz}\right)\Big|_{S_k} = \left(\sigma_{rr}^{(1)}n_{kr} + \sigma_{r\theta}^{(1)}n_{k\theta} + \sigma_{rz}^{(1)}n_{kz}\right)\Big|_{S_k},$$

$$\left(\sigma_{r\theta}^{(2k)}n_{kr} + \sigma_{\theta\theta}^{(2k)}n_{k\theta} + \sigma_{z\theta}^{(2k)}n_{kz}\right)\Big|_{S_k} = \left(\sigma_{r\theta}^{(1)}n_{kr} + \sigma_{\theta\theta}^{(1)}n_{k\theta} + \sigma_{z\theta}^{(1)}n_{kz}\right)\Big|_{S_k},$$

$$\left(\sigma_{rz}^{(2k)}n_{kr} + \sigma_{z\theta}^{(2k)}n_{k\theta} + \sigma_{zz}^{(2k)}n_{kz}\right)\Big|_{S_k} = \left(\sigma_{rz}^{(1)}n_{kr} + \sigma_{z\theta}^{(1)}n_{k\theta} + \sigma_{zz}^{(1)}n_{kz}\right)\Big|_{S_k},$$

$$u_r^{(2k)}\Big|_{S_k} = u_r^{(1)}\Big|_{S_k}, \quad u_\theta^{(2k)}\Big|_{S_k} = u_\theta^{(1)}\Big|_{S_k}, \quad u_z^{(2k)}\Big|_{S_k} = u_z^{(1)}\Big|_{S_k}, \quad k=1,2 \tag{7}$$

In the case considered, it is also assumed that the conditions

$$\sigma_{zz}^{(1)} \xrightarrow[|x_{20}|\to\infty]{} p, \quad \sigma_{(ij)}^{(1)} \xrightarrow[|x_{20}|\to\infty]{} 0 \quad (ij) \neq zz$$

$$\sigma_{(ij)}^{(2k)}(x_{1k},x_{2k},x_{3k}) = \sigma_{(ij)}^{(2k)}(x_{10}+kR_{12},x_{20},x_{30}) = \sigma_{(ij)}^{(20)}(x_{10},x_{20},x_{30}),$$

$$u_{(i)}^{(2k)}(x_{1k},x_{2k},x_{3k}) = u_{(i)}^{(2k)}(x_{10}+kR_{12},x_{20},x_{30}) = u_{(i)}^{(20)}(x_{10},x_{20},x_{30}),$$

$$\sigma_{(ij)}^{(1)}(x_{10},x_{20},x_{30}) = \sigma_{(ij)}^{(1)}(x_{10}+kR_{12},x_{20},x_{30}),$$

$$u_{(i)}^{(1)}(x_{10},x_{20},x_{30}) = u_{(i)}^{(1)}(x_{10}+kR_{12},x_{20},x_{30}) \tag{8}$$

are satisfied.

3. SOLUTION METHOD

To solve this problem, we use the boundary shape perturbation method developed in [3,6], according to which the unknown values are presented in series form in ε :

$$\left\{\sigma_{(ij)}^{(m)};\varepsilon_{(ij)}^{(m)};u_{(i)}^{(m)}\right\} = \sum_{q=0}^{\infty}\varepsilon^q\left\{\sigma_{(ij)}^{(m),q};\varepsilon_{(ij)}^{(m),q};u_{(i)}^{(m),q}\right\} ij=rr;\theta\theta;zz;r\theta;rz;\theta z, \ i=r;\theta;z \tag{9}$$

From Eqs. (4), we obtain a set of equations for each approximation (9). In this case, due to linearity, Eqs. (4)-(6) are satisfied for each approximation separately. Substituting Eqs. (9) into (7) and using Eqs. (3), after some manipulation described in [3,6], we obtain the contact conditions at $r_k = R$ for each approximation. We will present here these conditions for the zeroth and for the first approximations.

According to the investigations carried out and analyzed in [3-5], the main effect of the fibres curving on the stress distribution arises within the framework of the first approximation. The second and subsequent approximations give only some insignificant quantitative correction to these results. So we are here interested in the zeroth and in the first approximations.

If we write these conditions for the zeroth approximation and solve them by assuming that, the materials of the fibers are the same and their Poisson ratios are equal to that of the matrix material, then for the zeroth approximation, we have:

$$\sigma_{zz}^{(1),0} = p \; ; \; \sigma_{zz}^{(2k),0} = \sigma_{zz}^{(2),0} = \frac{E_3^{(2)}}{E_3^{(1)}}p \; ; \; \varepsilon_{zz}^{(2k),0} = \varepsilon_{zz}^{(1),0} = \frac{p}{E_3^{(1)}} \; ; \; u_z^{(2k),0} = u_z^{(1),0} = \varepsilon_{zz}^{(1),0}z \; ;$$

$$\sigma_{(ij)}^{(2k),0} = \sigma_{(ij)}^{(1),0} = 0 \; , \; k = -\infty,\dots,-2,-1,0,1,2,\dots,+\infty \; ; \; (ij) = rr, \theta\theta, r\theta, \theta z, rz \tag{10}$$

In Eqs. (13), $E_3^{(1)}$ and $E_3^{(2)}$ are the elastic moduli of the matrix and fiber materials, respectively, along the Oz axis.

After some calculations (given in [12]), for the first approximation we obtain an infinite system of algeabric equations for unknown constants as follows:

$$Y_n^{(1)k} + \sum_{v=0}^{\infty} \sum_{q=-\infty}^{+\infty} F_{nv}^{(1)q} Y_v^{(1)q} + F_n^{(2)k} Y_n^{(2)k} = 2\pi\delta_n^3 (\sigma_{zz}^{(1),0} - \sigma_{zz}^{(2),0}) \tag{11}$$

where $n = 0,1,2,...,\infty$, $\delta_3^3 = 1$ and $\delta_n^3 = 0$, if $n \neq 3$, $q = -\infty,...,k-1,k+1,...,+\infty$, $k = -\infty,...,-2,-1,0,1,2,...,+\infty$. The prime over the summations means that the case $q = k$ does not enter this summation. The quantities $D_{nv}^{(1)q}$, $F_{nv}^{(1)q}$ and $D_n^{(2)k}$, $F_n^{(2)k}$ are obtained from the above-considered corresponding formulas. Their detailed expressions are rather cumbersome and therefore are omitted here.

It follows from mechanical considerations and from the conditions (8) that

$$Y_n^{(1)-\infty} = ... = Y_n^{(1)-k} = ... = Y_n^{(1)0} = ... = Y_n^{(1)k} = ... = Y_n^{(1)\infty}$$

Thus, from Eqs. (11) we obtain

$$Y_n^{(1)0} + \sum_{v=0}^{\infty} Y_v^{(1)0} \left(\sum_{q=1}^{+\infty} 2F_{nv}^{(1)q} \right) + F_n^{(2)0} Y_n^{(2)0} = 2\pi\delta_n^3 (\sigma_{zz}^{(1),0} - \sigma_{zz}^{(2),0}) \tag{12}$$

For numerical investigations, the infinite system of algebraic equations (24) must be approximated by a finite system. To validate such a replacement, it must be shown that the determinant of the infinite system of equations is of normal type [11]: such is the case if we can prove the convergence of the series:

$$M = \sum_{n=0}^{\infty} \sum_{v=0}^{\infty} \left| \sum_{q=1}^{+\infty} F_{nv}^{(1)q} \right| \tag{13}$$

For investigating the series (13), we use the following asymptotic estimates of the functions $I_n(x)$ and $K_n(x)$:

$$I_n(x) < c_1 \frac{1}{n!} \left(\frac{|x|}{2} \right)^n, \ c_1 = \text{const.}, \ K_n(x) \approx c_2 (n-1)! \left(\frac{2}{|x|} \right)^n, \ c_2 = \text{const.} \tag{14}$$

These relations hold for large n and fixed x. Let

$$R/(R_{12} - 2L) > R/R_{12}, \ R_{12}/R > 2, \tag{15}$$

which means that the fibres do not have contact with each other. Then, taking into account Eqs. (14-15) and analysing the expressions of $F_{nv}^{(1)q}$, we obtain the following estimate for series (13):

$$M < c_3 \sum_{n=0}^{\infty} n^{c_4} (\rho - 1)^{-n}, \ c_3; c_4 = \text{const.}, \ \rho = R_{12} R^{-1}. \tag{16}$$

As the series on the right hand side converges, so does series (13). Note that such a proof was also performed in [2, 8-10]. Consequently, for numerical investigations the infinite system of algebraic equations (12) can be replaced by the following one:

$$Y_n^{(1)0} + \sum_{v=0}^{N_v} Y_v^{(1)0} \left(\sum_{q=1}^{N_q} 2F_{nv}^{(1)q} \right) + F_n^{(2)0} Y_n^{(2)0} = 2\pi\delta_n^3 (\sigma_{zz}^{(1),0} - \sigma_{zz}^{(2),0}), \ n = 1,2,...,N_v. \tag{17}$$

The values of N_ν and N_q in Eq. (17) are determined from the convergence requirement of numerical results.

It should be noted that in a similar manner we could determine the values of the second and subsequent approximations.

4. NUMERICAL RESULTS AND DISCUSSIONS

Let us assume that the materials of the fibers and matrix are isotropic with Young's moduli denoted by $E^{(2)}$ and by $E^{(1)}$, respectively. For the Poisson ratios ν, we assume that $\nu^{(1)} = \nu^{(2)} = 0.3$. We will investigate the normal stresses $\sigma_{\tau\tau}^{(1)}$ and $\sigma_{\tau\tau}^{(2)}$ which act along the fibers at influence points in matrix and in fibers respectively. In view of corresponding symmetry and periodicity, we consider the distribution of these stresses only on the surface S_0 (Figure 1).

If $\varepsilon = 0$ (i.e. the curving is absent), the stresses $\sigma_{\tau\tau}$ coincide with σ_{zz}.

Let us introduce the parameters $\kappa = 2\pi R / \ell$ and $\rho = R_{12} / R$. As it follows from the present investigations, the stress $\sigma_{\tau\tau}$ has a maximum at the point of S_0 which is determined from Eqs. (3) for $\theta_0 = \theta = 0$, $\alpha t_3 = \pi/2$.

Let us consider the graphs given in Figure 2. These graphs show the dependencies between the values of $\sigma_{\tau\tau}^{(1)} / \sigma_{33}^{(1)}$ and the parameter κ. Under obtaining these results it is assumed that $E^{(2)}/E^{(1)} = 50$, $\varepsilon = 0.015$, $N_\nu = 130$, $N_q = 17$. It follows from these graphs that the nonmonotonic character of the considered dependencies occurs for the row fibres. In this case the absolute values of $\sigma_{\tau\tau}^{(1)} / \sigma_{33}^{(1)}$ increase with increasing ρ. The results obtained for the row fibres and for a single fiber approach each other with $\rho \to \infty$.
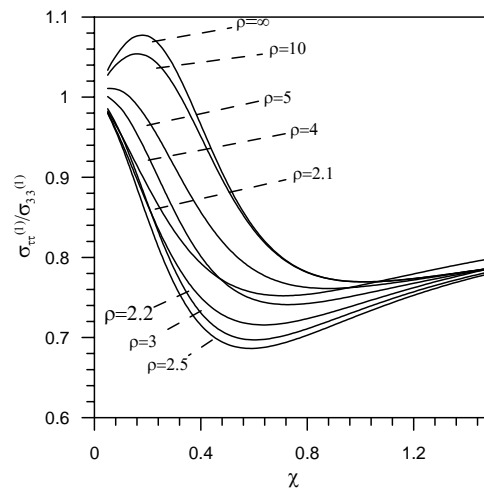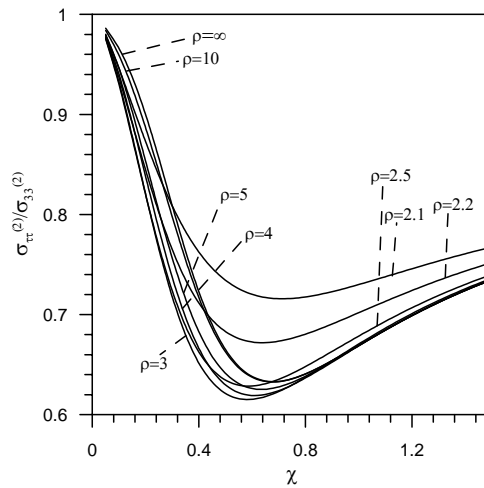

Figure 2. The graphs of the dependencies between $\sigma_{\tau\tau}^{(1)} / \sigma_{33}^{(1)}$ and κ for various values

of ρ for the case where $E^{(2)}/E^{(1)} = 50$, $\varepsilon = 0.015$

The graphs of the dependencies between $\sigma_{\tau\tau}^{(2)}/\sigma_{33}^{(2)}$ and the parameter κ under $E^{(2)}/E^{(1)} = 50$, $\varepsilon = 0.015$, $N_v = 130$, $N_q = 17$ are given in Figure 3. According to the results given in Figure 3, we can conclude that the values of $\sigma_{\tau\tau}^{(2)}/\sigma_{33}^{(2)}$ increase by decreasing ρ. Furthermore, these graphs show that the dependence between $\sigma_{\tau\tau}^{(2)}/\sigma_{33}^{(2)}$ and κ has a nonmonotonic character for all the values of ρ.

Note that, the results given in Figures 2 and 3 agree with the well-known mechanical considerations and coincide with the corresponding results obtained for the single fibre under $\rho \to \infty$ [3]. Consequently, these results validate the correctness of the algorithm and programmes used for numerical calculations.

Now we consider the graphs given in Figurs 4 and 5, which show the dependencies among $\sigma_{\tau\tau}^{(1)}/\sigma_{33}^{(1)}$, $\sigma_{\tau\tau}^{(2)}/\sigma_{33}^{(2)}$ and θ respectively under $\kappa = 0.7$, $E^{(2)}/E^{(1)} = 50$, $\alpha t_3 = \pi/2$, $\varepsilon = 0.015$, $N_v = 130$, $N_q = 17$. These graphs are constructed for various values of ρ. It follows from these graphs that $\sigma_{\tau\tau}(\pi/2 - \theta') = -\sigma_{\tau\tau}(\pi/2 + \theta')$, where $\theta' \in [0, \pi/2]$. These equalities agree with the periodicity of the structure of the considered material and with the curving form of the fibres.

Figure 3. The graphs of the dependencies between $\sigma_{\tau\tau}^{(2)}/\sigma_{33}^{(2)}$ and κ for various values of ρ for the case where $E^{(2)}/E^{(1)} = 50$, $\varepsilon = 0.015$

Consider some numerical results for the stresses $\sigma_{\tau\tau}^{(1)}/\sigma_{33}^{(1)}$ and $\sigma_{\tau\tau}^{(2)}/\sigma_{33}^{(2)}$ tabulated in Table 1. Note that these results are obtained for various $E^{(2)}/E^{(1)}$, ε and ρ under $N_v = 130$, $N_q = 17$. It follows from this table that the absolute values of the considered stresses decrease monotonically with $E^{(2)}/E^{(1)}$ and ε.
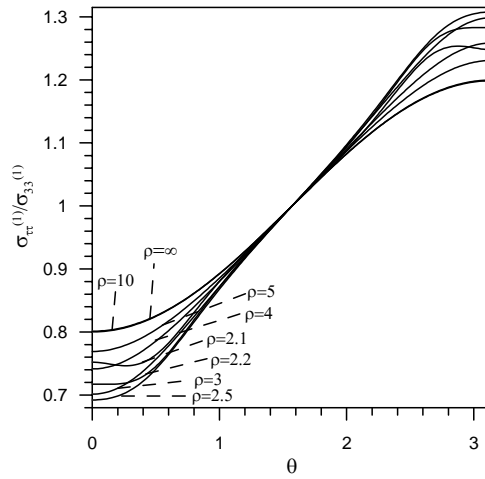
Figure 4. The graphs of the dependencies between $\sigma_{\tau\tau}^{(1)} / \sigma_{33}^{(1)}$ and θ for various values of ρ for the case where $E^{(2)}/E^{(1)} = 50$, $\varepsilon = 0.015$, $\kappa = 0.7$
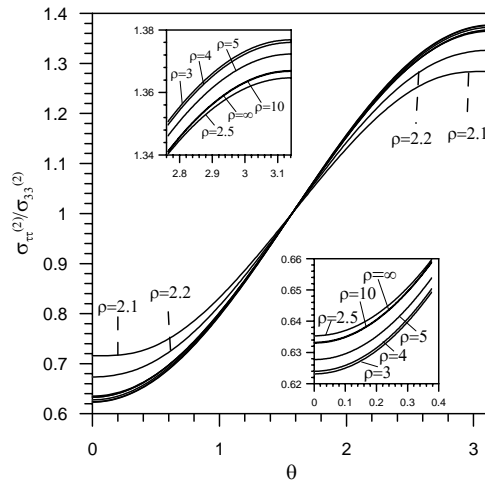

Figure 5. The graphs of the dependencies between $\sigma_{\tau\tau}^{(2)} / \sigma_{33}^{(2)}$ and θ for various values of ρ for the case where $E^{(2)}/E^{(1)} = 50$, $\varepsilon = 0.015$, $\kappa = 0.7$

The results given in Tables 2 and 3 show the convergence of the numerical results with respect to the values of N_q and N_v, respectively. Note that the values of N_q and N_v enter Eqs. (17). It is assumed that $\rho = 2.1$, $\varepsilon = 0.015$, $E^{(2)}/E^{(1)} = 50$, $N_v = 130$ (for the results

301

given in Table 2), $N_q = 17$ (for the results given in Table 3) from which it follows that the convergence of the solution method used is adequate.

Table 1. The values of $\sigma_{\tau\tau}^{(1)}/\sigma_{33}^{(1)}$ and $\sigma_{\tau\tau}^{(2)}/\sigma_{33}^{(2)}$ obtained for various ρ, $E^{(2)}/E^{(1)}$

and ε under $N_v = 130$, $N_q = 17$

$\dfrac{E^{(2)}}{E^{(1)}}$	ε	$\rho = 2.1$		$\rho = 2.5$		$\rho = 3.0$	
		$\dfrac{\sigma_{\tau\tau}^{(1),1}}{\sigma_{33}^{(1),0}}$	$\dfrac{\sigma_{\tau\tau}^{(2),1}}{\sigma_{33}^{(2),0}}$	$\dfrac{\sigma_{\tau\tau}^{(1),1}}{\sigma_{33}^{(1),0}}$	$\dfrac{\sigma_{\tau\tau}^{(2),1}}{\sigma_{33}^{(2),0}}$	$\dfrac{\sigma_{\tau\tau}^{(1),1}}{\sigma_{33}^{(1),0}}$	$\dfrac{\sigma_{\tau\tau}^{(2),1}}{\sigma_{33}^{(2),0}}$
10 (κ =1.1)	0.010	0.9365	0.9270	0.8997	0.8826	0.8940	0.8726
	0.015	0.9048	0.8905	0.8496	0.8239	0.8410	0.8090
	0.020	0.8730	0.8540	0.7995	0.7653	0.7880	0.7353
20 (κ =0.9)	0.010	0.9001	0.8255	0.8603	0.8352	0.8585	0.8255
	0.015	0.8502	0.8278	0.7905	0.7528	0.7878	0.7383
	0.020	0.8003	0.7704	0.7207	0.6704	0.7171	0.6511
50 (κ =0.7)	0.010	0.8347	0.8105	0.7947	0.7568	0.8008	0.7487
	0.015	0.7521	0.7158	0.6921	0.6353	0.7013	0.6231
	0.020	0.6695	0.6211	0.5894	0.5137	0.6017	0.4975
100 (κ =0.5)	0.010	0.7685	0.7352	0.7226	0.6711	0.7392	0.6642
	0.015	0.6528	0.6028	0.5839	0.5067	0.6088	0.4964
	0.020	0.5370	0.4705	0.4452	0.3423	0.4784	0.3235

Table 2. The convergence of the numerical results with respect to the values of N_q in

the case where $E^{(2)}/E^{(1)} = 50$, $\varepsilon = 0.015$, $\rho = 2.1$, $N_v = 130$

κ	stresses	The value of N_q					
		12	13	14	15	16	17
0.1	$\sigma_{\tau\tau}^{(1)}/\sigma_{33}^{(1)}$	0.9534	0.9533	0.9533	0.9532	0.9532	0.9532
	$\sigma_{\tau\tau}^{(2)}/\sigma_{33}^{(2)}$	0.9459	0.9460	0.9460	0.9460	0.9460	0.9460
0.2	$\sigma_{\tau\tau}^{(1)}/\sigma_{33}^{(1)}$	0.8890	0.8890	0.8890	0.8890	0.8890	0.8890
	$\sigma_{\tau\tau}^{(2)}/\sigma_{33}^{(2)}$	0.8727	0.8728	0.8728	0.8728	0.8728	0.8728
0.3	$\sigma_{\tau\tau}^{(1)}/\sigma_{33}^{(1)}$	0.8329	0.8329	0.8329	0.8329	0.8329	0.8329
	$\sigma_{\tau\tau}^{(2)}/\sigma_{33}^{(2)}$	0.8087	0.8087	0.8087	0.8087	0.8087	0.8087
0.4	$\sigma_{\tau\tau}^{(1)}/\sigma_{33}^{(1)}$	0.7926	0.7926	0.7926	0.7926	0.7926	0.7926
	$\sigma_{\tau\tau}^{(2)}/\sigma_{33}^{(2)}$	0.7625	0.7625	0.7625	0.7625	0.7625	0.7625

Table 3. The convergence of the numerical results with respect to the values of N_v in the case where $E^{(2)}\big/E^{(1)} = 50$, $\varepsilon = 0.015$, $\rho = 2.1$, $N_q = 17$

κ	stresses	The value of N_v						
		22	34	46	58	70	82	130
0.2	$\sigma_{\tau\tau}^{(1)}\big/\sigma_{33}^{(1)}$	0.8706	0.8833	0.8885	0.8894	0.8892	0.8890	0.8890
	$\sigma_{\tau\tau}^{(2)}\big/\sigma_{33}^{(2)}$	0.8662	0.8709	0.8722	0.8726	0.8727	0.8728	0.8728
0.3	$\sigma_{\tau\tau}^{(1)}\big/\sigma_{33}^{(1)}$	0.8103	0.8255	0.8317	0.8330	0.8329	0.8328	0.8329
	$\sigma_{\tau\tau}^{(2)}\big/\sigma_{33}^{(2)}$	0.7987	0.8058	0.8078	0.8083	0.8086	0.8086	0.8087
0.4	$\sigma_{\tau\tau}^{(1)}\big/\sigma_{33}^{(1)}$	0.7685	0.7843	0.7909	0.7924	0.7925	0.7924	0.7926
	$\sigma_{\tau\tau}^{(2)}\big/\sigma_{33}^{(2)}$	0.7506	0.7591	0.7614	0.7621	0.7623	0.7624	0.7625
0.5	$\sigma_{\tau\tau}^{(1)}\big/\sigma_{33}^{(1)}$	0.7442	0.7595	0.7659	0.7675	0.7678	0.7678	0.7679
	$\sigma_{\tau\tau}^{(2)}\big/\sigma_{33}^{(2)}$	0.7219	0.7306	0.7331	0.7338	0.7341	0.7342	0.7343

5. CONCLUSION

In the present paper, within the framework of the piecewise homogeneous body model with the use of the three-dimensional equations of the theory of elasticity for anisotropic body the method developed to investigate the stress distribution in the infinite elastic matrix containing a periodically curved row fibres having a sine-phase, is used to investigate related normal stresses which acting along the fibers at interface points. It is assumed that the materials of the fibres are the same and their midlines of the fibres are on the same plane. The numerical investigations have been made for the case where the materials of the fibres and matrix are both isotropic and homogeneous. According to the obtained numerical results it is established that the considered normal stresses related to matrix decrease, but the normal stress related to fiber increase with the fibres approaching each other.

REFERENCES

[1]   Tarnopolsky Yu.M., Jigun I.G. and Polyakov V.A., "Spatially-reinforced composite materials": Handbook, Mashinostroyenia, Moscow, 1987 (in Russian).
[2]   Guz A.N., "Failure mechanics of composite materials in compression". –Kiev: Naukova Dumka, 1990. –630 p. (in Russian.)
[3]   Akbarov, S.D. and Guz, A.N., "Mechanics of Curved Composites",-Kluwer Academic Publishers, 2000-464p.
[4]   Akbarov, S.D. and Guz, A.N., "Continuum approaches in the mechanics of curved composites and associated problems for structural members", Int. Appl. Mech., 2002, 38, N0:11, 1285-1305.
[5]   Akbarov, S.D. and Guz, A.N., "Mechanics of curved composites (piecewise homogenous body model)", Int. Appl. Mech., 2002, 38, N0:12, 1415-1439.
[6]   Akbarov, S.D. and Guz, A.N., "Method of Solving Problems in the Mechanics of Fiber Composites With Curved Structures", Soviet Applied Mechanics, -1985-March-p.777-785

[7]   Akbarov, S.D. and Guz, A.N., "Stress state of a fiber composite with curved structures with a low fiber concentration" Soviet Applied Mechanics. –1985-December-p.560-565.

[8]   Akbarov, S.D. and Kosker R., "Stress distribution caused by anti-phase periodical curving of two neighbouring fibers in a composite material", European Journal of Mechanics A/Solids, 2003, 22, 243–256.

[9]   Akbarov, S.D. and Kosker R., "On a stress analysis in the infinite elastic body with two neighbouring curved fibers" Composites Part B: Engineering, 2003, 34/2, 143-15.

[10]   Köşker R. and Akbarov, S.D., "Influence of the interaction between two neighboring periodically curved fibers on the stress distribution in a composite material" Mechanics of Composite Materials,2003, Vol.39, No. 2, 165-176.

[11]   Kantarovich, L.V. and Krilov, V.I., "Approximate methods in advanced calculus", Moscow: Fizmatgiz, 1962-708p. (in Russian).

[12]   Akbarov S.D., Kosker R. and Ucan., "Stress Distribution in the elastic body with periodically curved row fibers" , Mechanics of Composite Materials, 2004, Vol.40, No.3, 191-202.